Filamin A (FLNA) is required for cell–cell contact in vascular development and cardiac morphogenesis

Yuanyi Feng*†‡, Ming Hui Chen§¶, Ivan P. Moskowitz‖, Ashley M. Mendonza*†, Luis Vidali**, Fumihiko Nakamura**, David J. Kwiatkowski**††, and Christopher A. Walsh*†,††

*Division of Genetics and §Department of Cardiology, Children's Hospital Boston, Boston, MA 02215; †Beth Israel Deaconess Medical Center, Howard Hughes Medical Institute, and ‖Department of Genetics, Harvard Medical School, Boston, MA 02115; and Divisions of **Hematology and ¶Cardiology and Women's Health, Department of Medicine, Brigham and Women's Hospital, Boston, MA 02115

Communicated by Louis M. Kunkel, Harvard Medical School, Boston, MA, November 2, 2006 (received for review July 31, 2006)

Mutations in the human Filamin A (*FLNA*) gene disrupt neuronal migration to the cerebral cortex and cause cardiovascular defects. Complete loss of Flna in mice results in embryonic lethality with severe cardiac structural defects involving ventricles, atria, and outflow tracts, as well as widespread aberrant vascular patterning. Despite these widespread developmental defects, migration and motility of many cell types does not appear to be affected. Instead, Flna-null embryos display abnormal epithelial and endothelial organization and aberrant adherens junctions in developing blood vessels, heart, brain, and other tissues. Essential roles for FLNA in intercellular junctions provide a mechanism for the diverse developmental defects seen in patients with *FLNA* mutations.

adherens junctions | cardiovascular morphogenesis | angiogenesis | neural crest | neuronal migration

Filamin A (FLNA) is a widely studied actin binding protein whose specific cellular roles remain uncertain. First identified by its ability to cross-link actin filaments (1, 2), FLNA binds more than 30 diverse proteins (3, 4), but the physiological processes underlying these interactions are largely unclear. Human *FLNA* loss-of-function mutations cause periventricular heterotopia (PH), with abnormally migrated neurons present near the lateral ventricle, deep beneath their normal locations. PH is an X-chromosome-linked, male-lethal disease in which affected females have seizures (5–7). Because a FLNA-deficient cell line shows motility defects (8), PH has been interpreted as a cell-autonomous migratory arrest. Subsequently, specific *FLNA* missense alleles were associated with otopalatodigital syndromes 1 and 2, frontometaphyseal dysplasia and Melnick–Needles syndrome (9), although the effects of these missense alleles remain elusive.

Cardiovascular defects are increasingly associated with the loss of *FLNA* function in humans. Hemizygous males with *FLNA* mutations die prenatally or survive after birth with cardiac malformations, often dying postnatally from blood vessel rupture (5, 6, 10). PH patients also display congenital cardiovascular defects, such as patent ductus arteriosus, cardiac valvular anomalies, and a propensity for premature stroke or vascular disorders (11). Some patients also show Ehlers Danlos syndrome with vascular fragility and connective tissue defects, suggesting roles of FLNA in heart and vasculature.

Here we show that Flna-null mice die at midgestation with widespread hemorrhage from abnormal vessels, persistent truncus arteriosus (PTA), and incomplete cardiac septation. Conditional Flna knockout (KO) in the neural crest causes abnormalities of the cardiac outflow tract despite apparently normal migration of Flna-deficient neural crest cells. Moreover, Flna-null vascular endothelial cells display defects in cell–cell contacts. Our data suggest cell motility-independent functions of FLNA in cell–cell contacts and adherens junctions (AJs) during the development of many organs.

Results

Loss of Flna Results in Embryonic Lethality. Given the lethal effects of *FLNA* loss in human males, a conditional KO strategy was used with loxP sites inserted into introns 2 and 7 of the mouse *Flna* gene (Fig. 1*A*). Cre-mediated recombination deletes exons 3–7, producing a nonsense mutation with early Flna truncation at amino acid 121. Targeted ES cell clones transfected with a plasmid expressing Cre-recombinase-generated *Flna* floxed [or conditional KO ($Flna^c$)] and *Flna* KO alleles ($Flna^K$) confirmed by Southern and Northern blot analyses (Fig. 1 *B* and *C*). Western blot analyses with antisera to N- and C-terminal portions of FLNA detected no Flna protein in $Flna^{K/y}$ ES cells or $Flna^{K/y}$ embryos, whereas $Flna^{c/y}$ ES cells or embryos showed normal Flna levels (Fig. 1*D*). Two ES cell lines carrying $Flna^c$ alleles were injected into blastocysts to generate conditional $Flna^K$ mice. These mice were crossed with a β-actin Cre line to generate $Flna^{K/y}$ (Flna-null) mice. Breeding of *Flna* floxed $Flna^{c/c}$ females with β-actin Cre males gave rise to *Flna* heterozygous KO females ($Flna^{K/w}$) but no postnatal male progeny (of >100 wild-type and $Flna^{K/w}$ analyzed), suggesting that males lacking Flna died before birth.

Some $Flna^{K/w}$ females showed normal development, but ≈20% of $Flna^{K/w}$ females died in the first 3–4 months with many anomalies, including lung edema and emphysema, liver thrombi and necrosis, leukocytosis, and heart dilation (data not shown). $Flna^{K/w}$ females were very poor breeders. $Flna^{K/w}$ female mice were mated with C57BL/6 males, 24% of females at weaning age were $Flna^{K/w}$ (50% expected), confirming embryonic or early postnatal lethality in some $Flna^{K/w}$ heterozygotes (Table 1).

Vascular Defects in Flna-Null Mice. Male $Flna^{K/y}$ mice die by embryonic day (E)14.5 (Table 1) with vascular defects, including dilated s.c. vasculature, hemorrhage (Fig. 2*A*), and edema, suggesting abnormal vascular permeability. *In situ* hybridization at E9.5–E10.5 shows *FLNA* mRNA enriched in limb buds and intersomitic vessels (data not shown). Flna-null blood vessels were coarse and dilated, suggesting failure of vascular remodeling (Fig. 2 *A* and *C*). Immunostaining of E10.5 $Flna^{K/y}$ embryos with platelet–endothelial cell adhesion molecule (PECAM) revealed abnormal intersomitic blood vessels. Whereas normal intersomitic vessels do not penetrate somites (Fig. 2*B*), Flna-null blood vessels extended aberrant branches and sprouts into somitic tissues (Fig. 2*B*). PECAM immunostaining at E12 also

Author contributions: Y.F., D.J.K., and C.A.W. designed research; Y.F., I.P.M., A.M.M., and L.V. performed research; L.V. and F.N. contributed new reagents/analytic tools; Y.F., M.H.C., I.P.M., D.J.K., and C.A.W. analyzed data; and Y.F., D.J.K., and C.A.W. wrote the paper.

The authors declare no conflict of interest.

Freely available online through the PNAS open access option.

Abbreviations: AJ, adherens junction; E*n*, embryonic day *n*; F-actin, filamentous actin; FLNA, Filamin A; KO, knockout; PECAM, platelet–endothelial cell adhesion molecule; PH, periventricular heterotopia; PTA, persistent truncus arteriosus; VE-Cadherin, vascular endothelial-Cadherin; VSD, ventricular septal defect.

‡Present address: Department of Neurology, Center for Genetic Medicine, Northwestern University School of Medicine, Chicago, IL 60611.

††To whom correspondence may be addressed. E-mail: cwalsh@bidmc.harvard.edu or dk@rics.bwh.harvard.edu.

www.pnas.org/cgi/doi/10.1073/pnas.0609628104

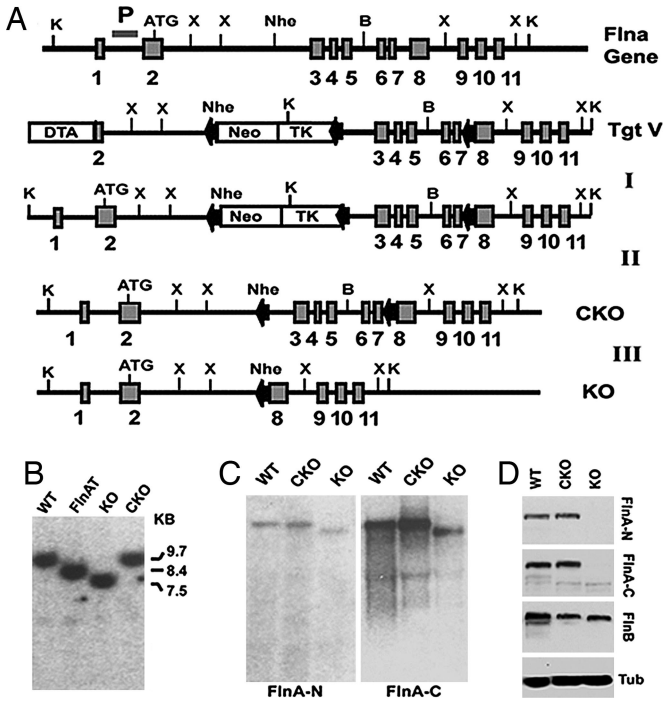

Fig. 1. Targeting strategy for Flna^c and null mutations. (*A*) A Neo-TK cassette flanked by loxP sites was inserted downstream of a 2.3-kb fragment containing exon 2 and intron 2 and upstream of an 8-kb fragment containing exons 3–11 of mouse Flna. A third loxP site was inserted into intron 7. The targeting vector was transfected into ES cells to generate Flna-targeted clones (Step I). Flna-recombinant ES cells were transfected with a Cre-recombinase-expressing plasmid, selected for ganciclovir resistance, and screened for deletion of the Neo-TK cassette alone (Step II) or with exons 3–7 of Flna (Step III). (*B*) A Southern blot analysis of Flna-targeted (FlnAT), FlnA^K, and Flna^c [conditional KO (CKO)] ES cells is shown. Genomic DNA was digested with KpnI. The Southern blot probe (P) is shown. The targeted Flna allele showed an 8.4-kb band instead of the 9.7-kb wild-type band. The 8.4-kb band reduced to 7.5 kb in the FlnA^K allele and to 9.7 kb in the conditional allele. (*C*) Northern blot analysis of Flna-null and conditional-null ES cells. The blot was probed with N- and C-terminal portions of Flna cDNA. FlnA^K cells showed a single Flna mRNA with deletion of exons 3–7. (*D*) An immunoblot of Flna mutant ES cells shows the deletion of Flna protein in the FlnA^K allele and unaltered Flna protein in the Flna^c allele (CKO). The blot was probed with antisera against peptides from mouse Flna N-terminal (anti-FLNA-N) and C-terminal (anti-FLNA-C) sequences. The blot was also probed with Flnb antiserum, which showed that Flnb expression is not increased in the absence of Flna. α-Tubulin (Tub) was used as loading control.

showed disorganized and exuberant blood vessels in Flna-null mutants (Fig. 2*C*). Nidogen immunostaining showed an intact basement membrane in mutant blood vessels at E14, but vessels were coarser and not remodeled into fine branches (Fig. 2*D*). Together, these data showed abnormal angiogenesis in Flna-null mice.

Severe Cardiac Defects in Flna-Null Mice. Flna-null mice showed prominent abnormalities of cardiovascular outflow tract and aortic arch, including PTA and interrupted aortic arch (in 13 of 13 Flna-null mice at E13.5–E14.5). The pulmonary artery and aorta originate as a common vessel and then septate into distinct outflow tracts arising from right and left ventricles, respectively. PTA constitutes a single "overriding" outflow tract spanning the two ventricles, an abnormal outflow tract valve, and a membranous ventricular septal defect (VSD) of the superior ventricular septum. At E12.5, *FLNA* mRNA is concentrated in the developing endocardial cushion, the cardiac outflow tracts, and the endothelial layer of blood vessels (Fig. 3*A*). Whole-mount images and H&E-stained sections showed a type I PTA with a single outflow tract overriding the right and left ventricles, an abnormally thickened and malformed outflow tract valve, incomplete septation of cardiac ventricles with a VSD, and the pulmonary artery arising from the truncal vessel (Fig. 3 *B* and *C*). The arch was interrupted between the left internal carotid and the left subclavian arteries, a type B interruption (Fig. 3*B*). More severe cardiac defects were seen in some Flna-null mice, with a single ventricle or with both atrial septal defect and VSD (Fig. 3*C*), demonstrating that Flna is essential for cardiac morphogenesis.

Migration-Independent Neural Crest Cell Defect. Because Flna is important in cell motility and migration, the cardiac defect may result from a migration defect of neural crest cells, which are essential for cardiac morphogenesis (12, 13). We used the Wnt1-Cre transgenic mouse (14) to excise the Flna^c allele selectively in neural crest. Flna$^{c/y}$ Wnt1-Cre$^+$ males showed milder defects than Flna$^{K/y}$ males and survived until birth in Mendelian ratios but died on the first postnatal day (Table 2) with cyanosis indicating hypoxemia (data not shown). All (seven of seven) Flna$^{c/y}$; Wnt1-Cre$^+$ males analyzed showed abnormal cardiac outflow tracts ranging from PTA to interrupted aortic arch type B, similar to Flna$^{K/y}$ mice, although less severe (Fig. 4 *A* and *B*). Thus, cell-autonomous defects in neural crest cells are partly responsible for cardiac and aortic defects in Flna-null mice.

To determine whether Flna-deficient neural crest cells were migrating normally, we introduced the ROSA26-LacZ Cre reporter allele into the Flna$^{c/c}$ mice (15) to mark Flna-deficient cells by expression of β-galactosidase. The Flna-deficient neural crest cells appeared to migrate normally with robust blue staining in all neural-crest-derived tissues, including endocardial cushion, cardiac outflow tract (Fig. 4 *C* and *D*), cranial vasculature, and brachial arch derivatives. LacZ staining and intensity in Flna$^{c/y}$ Wnt1-Cre$^+$ males was indistinguishable from wild-type and Flna$^{c/w}$ Wnt1-Cre$^+$ female controls; no aberrantly migrated or mislocalized stained cells were seen (Fig. 4 *C* and *D*), suggesting that abnormal migration of neural crest does not explain the cardiac defects in Flna mutants.

Normal Filamentous Actin (F-Actin) Structure, Motility, and Locomotion of Flna-Null Cells. Because Flna is required for the maintenance of F-actin in cell lines (8), we examined F-actin structure in cells from Flna-null mice. Sections of Flna-null mice stained with rhodamine phalloidin showed no differences in intensity

Table 1. Null mutation of Flna results in embryonic lethality

Genotype	E10.5–E11.5	E12.5	E13.5	E14.5	E15.5–E16.5	P0–P21
K/y	17	18	10(1d)	8(2d)	1(3d)	0
K/w	19	26	6	13	17	83
w/w + w/y	44	34	28	23	33	w/w,261;w/y,NC

Genotypes of embryos and pups from Flna heterozygous female and wild-type male crosses. K/y, Flna-null males; K/w, Flna heterozygous females; w/w, Flna wild-type females; w/y, Flna wild-type males; (*n*d), the number of dead embryos (not included in the main count) that were necrotic and partially resorbed; NC, not counted; P*n*, postnatal day *n*.

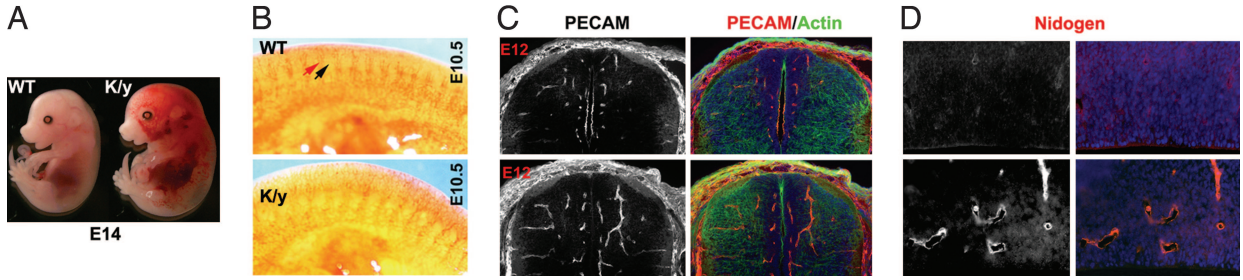

Fig. 2. Vascular defects in Flna-null mice. (*A*) A dying E14 Flna-null mutant embryo and wild-type littermate. Note the widespread hemorrhage, dilated blood vessels, and edema in the Flna-null (K/y) mouse. (*B*) Immunostaining of E10.5 mouse embryo with PECAM antiserum shows disorganization of vasculature in the Flna-null mice (K/y). The red arrow indicates intersomitic vessels, and the black arrow indicates somites. Boundaries between somites and intersomitic vessels are missing in the Flna-null mutant. (*C*) Immunostaining of a spinal cord with PECAM antiserum (in red) at E12. Note the abundant and exuberant blood vessels in an FlnA mutant. Sections are costained with FITC-conjugated phalloidin (for F-actin in green) and Hoechst (in blue). (*D*) Immunostaining of E14 cortical ventricular epithelium with antisera to Nidogen (in red). Blood vessels in the Flna-null brain are dilated but show intact basement membranes.

and structure of F-actin (data not shown). Flna-null mouse embryo fibroblasts showed normal stress fibers and focal adhesions revealed by Vinculin immunoreactivity (Fig. 5*A*) and normal motility and membrane ruffling (data not shown). Flna-null ES cells or neural progenitor cells differentiated *in vitro* into neurons with long axons and normal growth cones (Fig. 5*B*). Flna-null vascular endothelial cells showed normal intensity, architecture, and distribution of F-actin (Fig. 5*C*) and apparently normal filopodia and membrane protrusions (Fig. 5*C*), suggesting that Flna's essential roles may not relate to F-actin polymerization or cross-linking.

Cell–Cell Junction Defects of Flna-Null Endothelial Cells. Further analysis of Flna-null mice showed extensive defects in cell–cell junctions that were particularly well seen in vascular endothelial cells. PECAM immunostaining showed disorganized and discontinuous vascular endothelial cells in Flna-null mutants with irregular morphology (Fig. 6*A*, arrows). Vascular endothelial-Cadherin (VE-Cadherin) immunoreactivity, normally localized to AJs between vascular endothelial cells, was reduced or absent in Flna-null vessels (Fig. 6*B*), suggesting abnormal AJs and weakened cell–cell contacts. Ultrastructural analysis confirmed that mutant AJs were abnormal, being less electron-dense or unidentifiable, with excessive membrane ruffles at sites where AJs normally form (Fig. 6*C*). Abnormal AJs likely cause the hemorrhage and edema in mutants.

The widespread cardiac septation defect in Flna-null mice also appeared to result from aberrant endothelial cell organization in remodeling of the endocardial cushion. Wild-type endothelial cells at E12.5, labeled with NFATc1 and PECAM antibody, formed a continuous endothelial lining. In contrast, Flna-null endothelial cells were poorly organized, with clusters or multiple layers and gaps in both the endocardial cushion and outflow tract (Fig. 6*D*). F-actin, cell proliferation, and mesenchymal organization appeared normal in the mutant (data not shown), consistent with abnormal organization of endothelial cells in Flna-null mice.

Flna in Brain Development. The defective cell–cell contacts not only are central to the cardiovascular defects in Flna mutants, they also provide a plausible explanation for the heterotopic neurons lining the ventricle in humans with *FLNA* mutations. The Flna protein showed a polarized localization at the ventricular surface, where neuroepithelial cells are connected by AJs (Fig. 7*A*) (16), analogous to its localization in endothelial cells. Although α-catenin, β-catenin, zonula occludens-1, and F-actin were normally distributed (Fig. 7*B* and data not shown), VE-Cadherin (Cadherin 5) lost its normal localization in Flna-null progenitors (Fig. 7*B*). Analysis of Flna-null males was limited due to early lethality, but a few surviving E14.5 mutants showed a smaller but grossly normal brain with a thinner cortical plate that was normally positioned (Fig. 7*C*). Flna-null neurons were not arrested in the ventricular zone, and at least some migrated to the cortical plate by E14.5, with no heterotopic neurons observed (Fig. 7*D*). The lack of migratory arrest, together with the aberrant VE-Cadherin localization in Flna-null neuroepi-

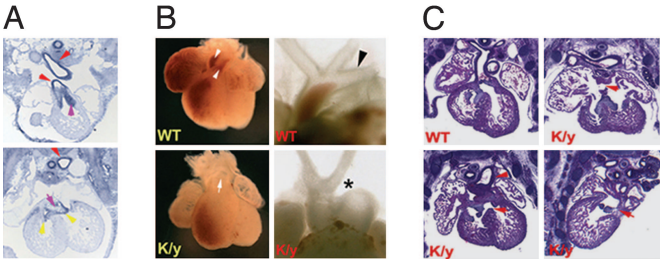

Fig. 3. Cardiac morphogenesis defects caused by Flna deficiency. (*A*) Flna expression in E12.5 mouse embryos is seen in the endocardial cushion (pink arrowheads); outflow tract (red arrowheads); and cardiac valves (yellow arrowheads). (*B*) Heart images of Flna-null (K/y) and wild-type littermates at E13.5 show the single outflow tract (PTA, indicated by the arrow) in the K/y mice. The K/y heart displayed PTA and interrupted aortic arch type B, with interruption between the left internal carotid artery and left subclavian artery (asterisk). Wild-type hearts show a normal aortic arch (arrowheads). (*C*) H&E-stained coronal sections of an Flna mutant heart (K/y) and of wild-type (*Upper Left*) littermates at E13.5. All Flna mutant embryos displayed incomplete septation of the ventricles (VSD, arrows) and outflow tracts (PTA, arrowhead). A single ventricle is seen (*Upper Right*), and combined atrial septal defect–VSD is seen (*Lower Right*).

Table 2. Flna neural crest conditional knockout mice (c/y Wnt-Cre) die at birth

Age	c/y Cre$^+$	c/w Cre$^+$	c/y Cre$^-$; c/w Cre$^-$	Total/ no. of litters
E17.5–E18.5	21	21	48	90/7
P0	13(6d)	26	30	69/7
P1–P1.5	0	41	57	98/11

Genotypes of embryos and postnatal pups from crosses between homozygous Flna floxed (Flna$^{c/c}$) females and Wnt1-Cre males. c/y Cre$^+$, conditional Flna Wnt1-Cre mutant males; c/w Cre$^+$, conditional Flna Wnt1-Cre mutant females; c/y Cre$^-$ and c/w Cre$^-$, conditional Flna mice that lack Cre recombinase; (*n*d), number of dead pups (not included in the main count); P*n*, postnatal day *n*.

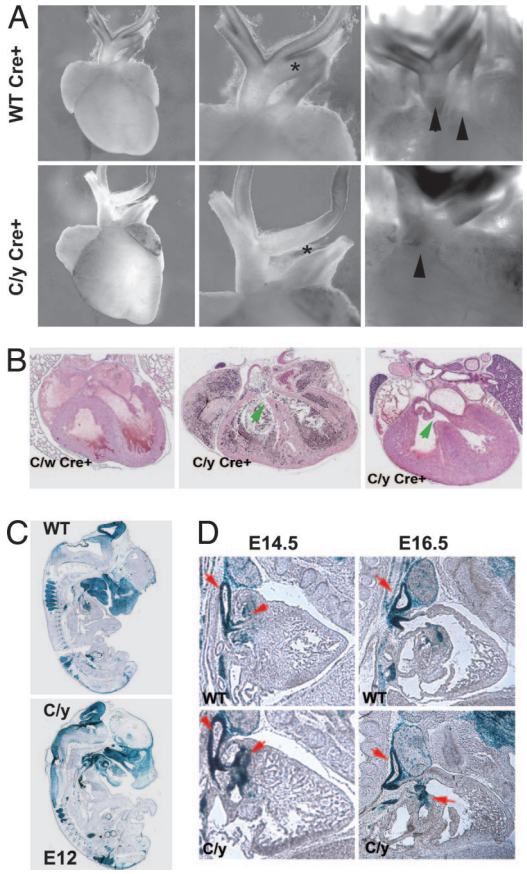

Fig. 4. Migration-independent neural crest defect in cardiac morphogenesis. (*A*) Heart images of Flna Wnt1-cre mutant males (C/y Cre+) and wild-type or heterozygous female litter mates. C/y Cre+ animals display PTA and interrupted aortic arch type B, with interruption between the left internal carotid artery and left subclavian artery (asterisk). (*B*) Pathological analysis (H&E stain) demonstrated that the outflow tract of male Wnt1-Cre Flna^c mice (c/y Cre+) failed to septate, resulting in PTA (arrows). (*C* and *D*) Fate mapping of neural crest cells using ROZA26LacZ Cre reporter, in which the Flna mutant cells were visualized by expression of β-galactosidase. At E12.5, E14.5, and E16.5, Flna-deficient cells distribute normally in neural-crest-derived tissues, including the cardiac outflow tract and endocardial cushion (red arrows).

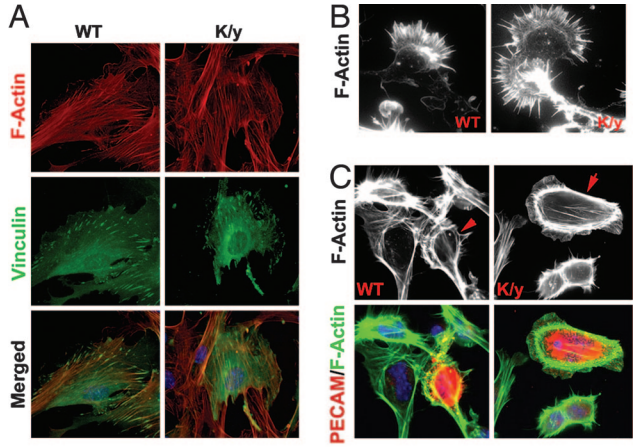

Fig. 5. Normal F-actin structure, motility, and locomotion of Flna-null cells. (*A*) The immunofluorescence of mouse embryo fibroblasts from Flna-null embryos and littermates at E12.5. Cells were stained with a monoclonal antibody to Vinculin (in green) and costained with rhodamine-conjugated phalloidin (in red), and Hoechst (in blue). (*B*) The immunofluorescence of Flna-null neurons derived by differentiation of Flna-null ES cells with 0.5 μM retinoic acid or from cortical neural progenitor cells. Cells were stained with rhodamine-conjugated phalloidin to visualize F-actin in the neuronal growth cone. Cytoskeletal structures in Flna-null neurons are indistinguishable from wild-type neurons. (*C*) Flna-deficient endothelial cells identified by PECAM immunostaining (in red). F-actin intensity and structure visualized with FITC-conjugated phalloidin are similar in Flna-null and wild-type cells.

thelial cells, suggests that a loss of AJs in the brain may create periventricular nodules due to disruption of the ventricular lining (17, 18).

Discussion

We show that a loss of Flna results in disorganized vasculature, defective blood vessels, misshapen endothelial cells, and abnormal AJs, with widespread edema, hemorrhage, and embryonic death. Flna-null embryos showed cardiac morphogenesis abnormalities involving septation failure of ventricles, atria, and outflow tracts, leading to PTA, VSDs, and atrial septal defects. The outflow tract defect in Flna-null embryos appears to result partially from abnormal neural-crest-derived cells because ablation of Flna in neural crest cells alone impairs outflow tract remodeling, whereas lack of Flna in non-neural-crest cells likely also contributes to these defects. Surprisingly, the morphogenesis defects seen with Flna mutation are not associated with detectable defects in F-actin stability, cell motility, or migration in a variety of cell types. Rather, abnormal cell junctions in Flna mutant cells suggest an unexpected role for Flna in AJs.

FLNA and AJs. Despite literature linking Flna to migration (4), the most striking cellular defect in Flna mutants is aberrant AJs. Along with structural defects of AJs, reduced AJ protein VE-Cadherin was seen in vascular endothelial cells and in neuroepithelial cells. By regulating endothelial cell growth and contact inhibition, paracellular permeability, and homophilic cell–cell adhesion, AJs are essential for the organization of vessels during angiogenesis (19). Stable AJs require integration of cell surface proteins with intracellular partners that anchor the actin cytoskeleton. Flna may stabilize F-actin at AJs, or it may connect membrane molecules to cytoskeletal complexes. Although Flna deficiency alters VE-Cadherin, we did not observe changes in other components of AJs, such as α- and β-catenins, the tight junction protein zonula occludens-1, or other membrane molecules, such as ephrin B (data not shown). Therefore, Flna may act in parallel with catenins to allow AJ molecules to signal to the actin cytoskeleton or may act as a molecular switch to regulate actin dynamics at AJs. Although we cannot exclude that other membrane molecules are also altered by Flna mutation, the reduced VE-Cadherin in blood vessels and neuroepithelial cells suggests a role of Flna in AJs.

The role of Flna in AJs links early, hemorrhagic phenotypes and late vascular phenotypes of FLNA deficiency. Severe incompetence of vascular AJs leads to early defects in vascular patterning and integrity. On the other hand, *FLNA* heterozygous females generally survive embryonic development but are subject to postnatal vascular syndromes, including early onset stroke and aortic dissection (6). Because *FLNA* heterozygous females are mosaics of cells expressing and not expressing FLNA due to the X chromosome location of the gene, mosaic dysfunction in Flna-null endothelial cells in females could explain the variable clinical features.

Flna in Cardiac Morphogenesis. Flna is one of three filamin isoforms essential for normal development in humans (6, 9, 20, 21). Flnb has some overlapping expression with Flna and could provide functional redundancy in some cell types (22, 23). Although Flnc is fairly specific to muscle cells (24), it expresses in some nonmuscle cells during development (data not shown).

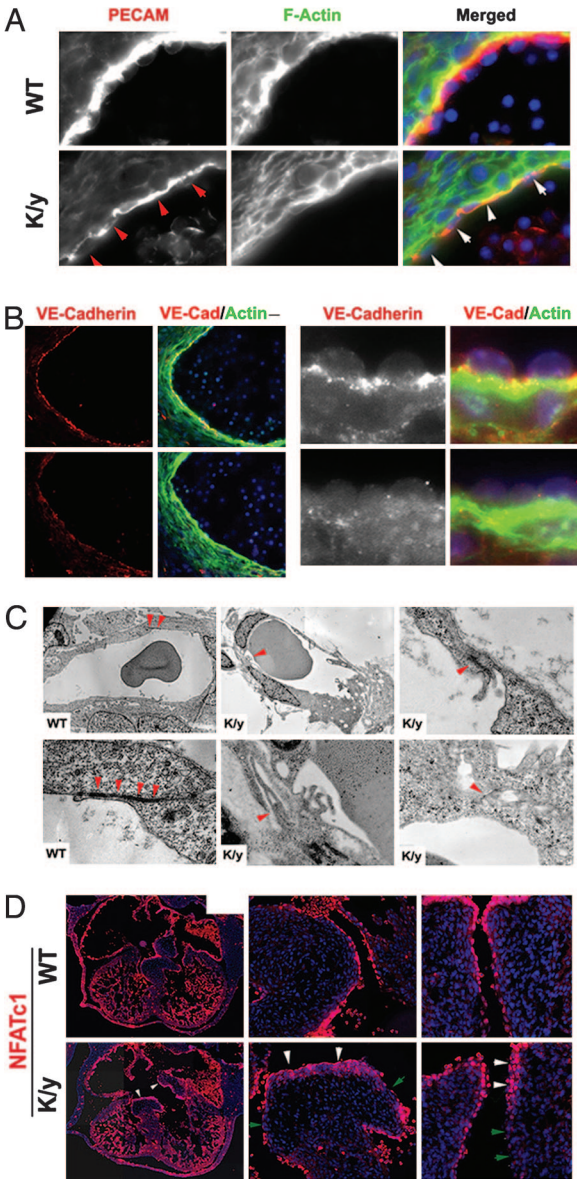

Fig. 6. Defective AJs in Flna-deficient vascular endothelial cells. (*A* and *B*) Immunostaining with PECAM and VE-Cadherin antibodies showing that blood vessel endothelial cells are abnormally organized and that the intensity and distribution of VE-Cadherin are altered in the Flna-null mice at E12.5. Sections were costained with FITC-conjugated phalloidin (green) and Hoechst (blue). Arrows show disorganized and atrophic endothelial cells. (*C*) The transmission electron micrographs of capillary endothelial cells from Flna-null mice (K/y) and wild-type littermates. Arrowheads indicate AJs between neighboring cells. Note that the AJs in K/y endothelial cells are malformed with reduced electron density. (Magnification: ×1,000 or ×2,500, respectively.) (*D*) Defective endothelial cell organization in Flna-null hearts. Sections of developing hearts from Flna-null embryos and wild-type littermates at E12.5 show endothelial cells labeled with a monoclonal antibody to NFATc1 (in red). White arrowheads show endothelial cell clusters or multiple layers; green arrowheads indicate regions with absent or defective endothelial lining.

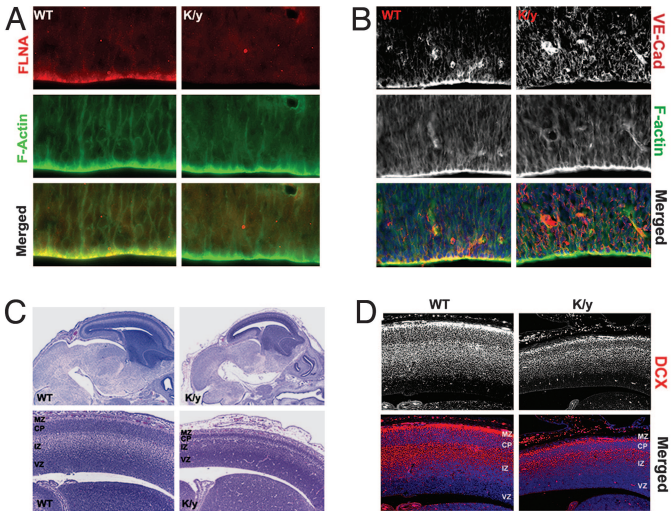

Fig. 7. Brain development defects of Flna-null mice. (*A*) Immunostaining with a monoclonal antibody to Flna shows that Flna is concentrated at the apical surface of neuroepithelial cells in developing cerebral cortex. (*B*) Immunostaining with VE-Cadherin antibody (red) indicated its absence from the apical surface of the epithelial cells in cerebral cortex of Flna-null mice at E12.5. Sections also were costained with FITC-conjugated phalloidin (in green) and Hoechst (in blue). (*C*) Histological analysis of Flna-null mice (E14.5–E15) shows that the mutant brain was smaller, with reduced thickness in cortical plate and dilated blood vessels. (*D*) Immunostaining with Doublecortin (DCX) antiserum showed newly generated cortical neurons in the intermediate zone and cortical plate in Flna-null and wild-type brain, with no accumulation of neurons in cortical ventricular zone in Flna-null mutant. VZ, ventricular zone; IZ, intermediate zone; CP, cortical plate; MZ, marginal zone.

Nonetheless, loss of Flna alone results in severe defects in the heart and blood vessels, suggesting that Flna is essential for cardiovascular morphogenesis.

Flna's role in heart morphogenesis may involve multiple cell types. Loss of Flna in the neural crest disrupted cardiac outflow tracts, suggesting a cell-autonomous role of Flna in neural crest. Although failure of outflow tract septation is a hallmark of the ablation of premigratory neural crest cells (12, 13), Flna-deficient neural crest cells showed apparently normal migration and targeting into the distal endocardial cushion. Therefore, our data demonstrate an Flna-dependent, postmigratory mechanism that is essential for the differentiation and remodeling of neural crest derivatives after they reach the target tissue.

Because Flna-null hearts are more severely malformed than Flna Wnt1-Cre mutants, Flna has critical functions in non-neural-crest cells as well as neural crest cells. Flna is expressed highly in endothelial cells and endocardial cushion mesenchymal cells, and Flna deficiency appears to affect the development of the endocardial cushion, which normally generates the uppermost segment of the interventricular septum. The disorganized endothelial cells in the endocardial cushion in Flna-null mutants suggest that Flna plays a role either in organizing endothelial cells or in the interaction of endothelial and mesenchymal cells.

Flna in Brain Development. The requirement of Flna in AJs provides an unexpected explanation for its roles in other tissues, notably in brain. The localization of Flna at AJs between neuroepithelial cells suggests that defects in AJs, rather than requirements in migration, produce the accumulation of neurons at the ventricular surface in humans with *FLNA* mutations. This hypothesis is supported by the loss of the normal localization of VE-Cadherin in Flna-null mice and by cases of males with *FLNA* mutations (6, 7, 10). These males, some of which are born to mothers with heterozygous *FLNA* mutations and who are hence not somatic mosaics, show that many *FLNA* mutant neurons successfully migrated to the cerebral cortex (10). Similarly, viable $Flna^{K/w}$ mice showed no neuronal heterotopia at 1–3 months of age. Nonetheless, ≈50% of $Flna^{K/w}$ mice died before weaning and variably to the extent of the contribution of Flna-null cells to various tissues, including brain, may contribute to this poor survival. Mutations in αSnap and ARFGEF2 also

result in periventricular neuronal nodules in mice and humans, respectively (18, 25, 26), and both are required for membrane trafficking. As neuroepithelial cell polarity regulates progenitor cell fate (18, 27), defects of cell polarity and adhesion due to Flna deficiency may alter progenitor proliferation and neurogenesis and lead to the ectopic neuronal nodules in PH patients as well as cytoarchitectural defects of cerebral cortex seen in some males with *FLNA* mutations (10).

Methods

Flna Mutant Mice. Genomic fragments containing exon 2 to intron 2 (2.3 kb) and exons 3–11 (8 kb) of the mouse Flna gene were cloned into a loxP targeting vector (28). A loxP site was inserted into intron 7. Gene targeting in 129SvEv J1 ES cells was performed as described (28). Two positive, karyotyped clones were transfected with a Cre recombinase plasmid as described (28) and screened for deletion of the Neo-TK cassette alone or with exon 3–7 of Flna. Two $Flna^{c}$ clones were injected into C57BL/6 blastocysts. Germ-line males crossed with wild-type C57BL/6 females yielded heterozygous Flna floxed females, which were crossed with β-actin Cre males followed with wild-type C57BL/6 males to generate Flna heterozygous ($Flna^{K/w}$) mice. $Flna^{K/w}$ mice were bred with wild-type C57BL/6 males; one-fourth of the offspring is predicted to be an Flna-null male.

Histology and Immunohistochemistry and Antibodies. Timed embryos (E10–E17) were fixed with 4% paraformaldehyde. Paraffin sections were stained with H&E. Frozen sections were analyzed with antibodies to PECAM, VE-Cadherin, NFATc1 (BD Pharmingen, San Diego, CA), Nidogen (Calbiochem, San Diego, CA), Doublecortin (29), α-smooth muscle actin (DCX and αSMA, respectively; Sigma, St. Louis, MO), phosphohistone H3 (Upstate, Billerica, MA), Flnb, and Flna (kindly provided by T. Stossel and J. Hartwig) (30). At least three mutant and three wild-type littermates were analyzed. *In situ* hybridization and staining of E10.5 embryos with anti-PECAM/CD31 monoclonal antibody MEC13.3 (BD Pharmingen) were performed as described (23, 31).

Cell Culture and Immunostaining. Primary mouse embryo fibroblast lines were immortalized from E12–E13 mouse embryos (32) and analyzed in early passages (before postnatal day 5). Primary vascular endothelial cells from E10 mouse embryos were digested with 0.25% trypsin; plated on extracellular matrix gel (Sigma); cultured overnight in Ham's F12K medium with 10% FBS, 0.1 mg/ml heparin, and 5 μg/ml endothelial cell growth supplement (Sigma); and stained as described (6). Neural progenitors isolated from E13 cerebral cortex were cultured as neurospheres and differentiated into neurons as described (33).

Note. During the submission of this work, the *Dilp2* mouse mutant with a Flna point mutation that truncates the protein at Ig-like repeat 22 was reported with cardiac defects (30), although vascular defects were not reported. The *Dilp2* mutant showed normal recruitment of cardiac neural crest cells, but the postmigratory role of Flna in neural crest was not shown. However, our findings of defective cell–cell contacts provide a mechanism underlying the functions of *FLNA* and form a unifying hypothesis for its roles in human disease.

The authors thank Drs. T. Stossel and J. Hartwig (Brigham and Woman's Hospital) for many helpful discussions, Flna antibodies, and critical readings of the manuscript; Dr. R. Bronson for histology; Drs. C. Seidman and J. Seidman for helpful discussions and advice; Dr. J. Corbo and D. Graham for library screening; K. Heiberger for gene targeting; Dr. A. Sharp and L. Du (Brigham and Women's Hospital) for ES cell and blastocyst injections; and members of the Walsh laboratory for help. This work was supported by National Institute of Neurological Disorders and Stroke Grant P01NS40043 (to C.A.W.). C.A.W. is an Investigator of the Howard Hughes Medical Institute. Y.F. was supported by National Institute of Mental Health Career Development Award K01MH065338.

1. Hartwig JH, Tyler J, Stossel TP (1980) *J Cell Biol* 87:841–848.
2. Gorlin JB, Yamin R, Egan S, Stewart M, Stossel TP, Kwiatkowski DJ, Hartwig JH (1990) *J Cell Biol* 111:1089–1105.
3. Feng Y, Walsh CA (2004) *Nat Cell Biol* 6:1034–1038.
4. Stossel TP, Condeelis J, Cooley L, Hartwig JH, Noegel A, Schleicher M, Shapiro SS (2001) *Nat Rev Mol Cell Biol* 2:138–145.
5. Eksioglu YZ, Scheffer IE, Cardenas P, Knoll J, DiMario F, Ramsby G, Berg M, Kamuro K, Berkovic SF, Duyk GM, *et al*. (1996) *Neuron* 16:77–87.
6. Fox JW, Lamperti ED, Eksioglu YZ, Hong SE, Feng Y, Graham DA, Scheffer IE, Dobyns WB, Hirsch BA, Radtke RA, *et al*. (1998) *Neuron* 21:1315–1325.
7. Sheen VL, Dixon PH, Fox JW, Hong SE, Kinton L, Sisodiya SM, Duncan JS, Dubeau F, Scheffer IE, Schachter SC, *et al*. (2001) *Hum Mol Genet* 10:1775–1783.
8. Cunningham CC, Gorlin JB, Kwiatkowski DJ, Hartwig JH, Janmey PA, Byers HR, Stossel TP (1992) *Science* 255:325–327.
9. Robertson SP, Twigg SR, Sutherland-Smith AJ, Biancalana V, Gorlin RJ, Horn D, Kenwrick SJ, Kim CA, Morava E, Newbury-Ecob R, *et al*. (2003) *Nat Genet* 33:487–491.
10. Guerrini R, Mei D, Sisodiya S, Sicca F, Harding B, Takahashi Y, Dorn T, Yoshida A, Campistol J, Kramer G, *et al*. (2004) *Neurology* 63:51–56.
11. Moro F, Carrozzo R, Veggiotti P, Tortorella G, Toniolo D, Volzone A, Guerrini R (2002) *Neurology* 58:916–921.
12. Kirby ML, Waldo KL (1995) *Circ Res* 77:211–215.
13. Stoller JZ, Epstein JA (2005) *Semin Cell Dev Biol* 16:704–715.
14. Danielian PS, Echelard Y, Vassileva G, McMahon AP (1997) *Dev Biol* 192:300–309.
15. Zambrowicz BP, Imamoto A, Fiering S, Herzenberg LA, Kerr WG, Soriano P (1997) *Proc Natl Acad Sci USA* 94:3789–3794.
16. Chenn A, Zhang YA, Chang BT, McConnell SK (1998) *Mol Cell Neurosci* 11:183–193.
17. Zhang LL, Collier PA, Ashwell KW (1995) *Neurotoxicol Teratol* 17:297–311.
18. Chae TH, Kim S, Marz KE, Hanson PI, Walsh CA (2004) *Nat Genet* 36:264–270.
19. Bazzoni G, Dejana E (2004) *Physiol Rev* 84:869–901.
20. Krakow D, Robertson SP, King LM, Morgan T, Sebald ET, Bertolotto C, Wachsmann-Hogiu S, Acuna D, Shapiro SS, Takafuta T, *et al*. (2004) *Nat Genet* 36:405–410.
21. Vorgerd M, van der Ven PF, Bruchertseifer V, Lowe T, Kley RA, Schroder R, Lochmuller H, Himmel M, Koehler K, Furst DO, Huebner A (2005) *Am J Hum Genet* 77:297–304.
22. Takafuta T, Wu G, Murphy GF, Shapiro SS (1998) *J Biol Chem* 273:17531–17538.
23. Sheen VL, Feng Y, Graham D, Takafuta T, Shapiro SS, Walsh CA (2002) *Hum Mol Genet* 11:2845–2854.
24. Chakarova C, Wehnert MS, Uhl K, Sakthivel S, Vosberg HP, van der Ven PF, Furst DO (2000) *Hum Genet* 107:597–611.
25. Bronson RT, Lane PW (1990) *Brain Res Dev Brain Res* 54:131–136.
26. Sheen VL, Basel-Vanagaite L, Goodman JR, Scheffer IE, Bodell A, Ganesh VS, Ravenscroft R, Hill RS, Cherry TJ, Shugart YY, *et al*. (2004) *Brain Dev* 26:326–334.
27. Klezovitch O, Fernandez TE, Tapscott SJ, Vasioukhin V (2004) *Genes Dev* 18:559–571.
28. Feng Y, Walsh CA (2004) *Neuron* 44:279–293.
29. Gleeson JG, Lin PT, Flanagan LA, Walsh CA (1999) *Neuron* 23:257–271.
30. Nakamura F, Pudas R, Heikkinen O, Permi P, Kilpelainen I, Munday AD, Hartwig JH, Stossel TP, Ylanne J (2006) *Blood* 107:1925–1932.
31. Schlaeger TM, Qin Y, Fujiwara Y, Magram J, Sato TN (1995) *Development (Cambridge, UK)* 121:1089–1098.
32. Todaro GJ, Green H (1963) *J Cell Biol* 17:299–313.
33. Galli R, Gritti A, Bonfanti L, Vescovi AL (2003) *Circ Res* 92:598–608.